

# Elastic Convection in Vibrated Viscoplastic Fluids

Hayato Shiba<sup>1,2</sup>, Jori Ruppert-Felsot<sup>1</sup>, Yoshiaki Takahashi<sup>1</sup>, Yoshihiro Murayama<sup>1</sup>, Qi Ouyang<sup>3</sup>, Masaki Sano<sup>1</sup>

<sup>1</sup>Department of Physics, <sup>2</sup>Department of Applied Physics, University of Tokyo,  
Hongo, Bunkyo-ku, Tokyo <sup>1</sup>113-0033, <sup>2</sup>113-8656, Japan and

<sup>3</sup>Department of Physics and Mesoscopic Physics Laboratory, Peking University, Beijing 100871, China  
(Dated: November 15, 2018)

We observe a new type of behavior in a shear thinning yield stress fluid: freestanding convection rolls driven by vertical oscillation. The convection occurs without the constraint of container boundaries yet the diameter of the rolls is spontaneously selected for a wide range of parameters. The transition to the convecting state occurs without hysteresis when the amplitude of the plate acceleration exceeds a critical value. We find that a non-dimensional stress, the stress due to the inertia of the fluid normalized by the yield stress, governs the onset of the convective motion.

PACS numbers: 47.54.-r, 47.55.P-, 89.75Kd

Complex fluids comprise a large number of fluids in everyday and industrial usage. Viscoelastic fluids often exhibit interesting behavior when subjected to mechanical stresses, such as rod climbing and the open siphon effect[1, 2]. Viscoplastic fluids that possess a yield stress can exhibit both elastic solid-like behavior and fluid-like behavior. Thus a blob of viscoplastic fluid can retain its shape when laid on a plate, even if turned upside down, if the stress due to its own weight does not exceed the yield stress. With the application of a mechanical shear stress larger than the yield stress, resistance to the stress abruptly decreases and the fluid starts to flow or falls in drops. In the present work, we observe a new instability that arises in soft yield stress fluids driven far from equilibrium that reveals characteristics particular to plastic flow which is not observed in various pattern formation in non-Newtonian fluids[3, 4] without yield stress.

Vibrated materials often show a variety of patterns such as Faraday's surface waves in Newtonian fluids, stripe and labyrinthine patterns and convection of granular materials[5, 6], and localized excitation of shear-thickening fluids[7]. The convection of vibrated viscoplastic fluids observed in the present work is a new example of pattern forming instabilities of vibrated materials. In many pattern-forming systems, the evolution of the pattern can occur on a timescale much slower than that of the forcing. Understanding how the slow mode of the pattern dynamics emerges from the fast excitation mode is a fundamental problem in the nonlinear dynamics of far from equilibrium systems.

When a viscoplastic fluid placed on a horizontal plate is vertically vibrated, freestanding convective rolls appear as a lip shape, as shown in Fig. ???. We observe that a pair of rolls is spontaneously created, and counter-rotate with a slow circulation speed independent of the fast vibrating mode of the plate. The convection rolls are freely standing on the horizontal surface without side and top boundary walls. The diameter of the rolls is spontaneously selected and not determined by the depth of the container. This is in contrast to thermal convec-

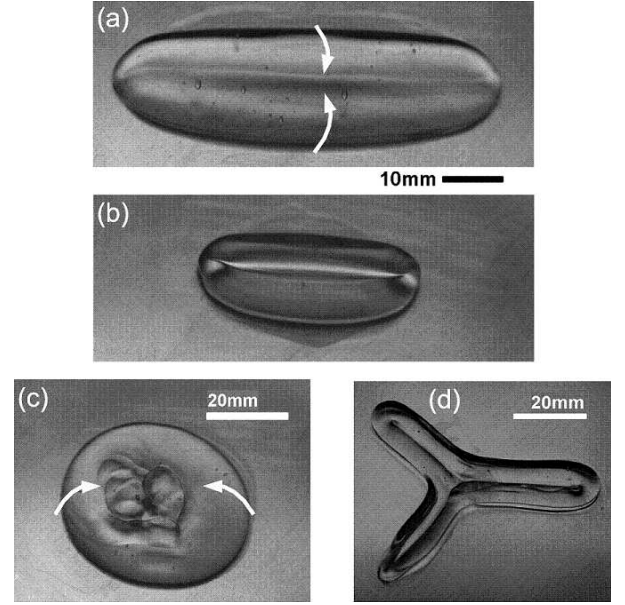


FIG. 1: (a) Overhead view of the convecting rolls on a horizontal plate (R1 gel), vertically vibrated at  $f = 40$  Hz and acceleration amplitude  $\Gamma = 11.1$ . The volume of the gel used was  $V = 6$  mL. (b) Resulting roll pattern using a smaller volume,  $V = 3$  mL, at  $f = 40$  Hz,  $\Gamma = 12.0$ . The scale bar is the same as that of (a). (c) Ring pattern obtained at higher volumes. The mean convecting flow occurs in the outer ring region.  $f = 40$  Hz,  $\Gamma = 15.0$ , and  $V = 9$  mL. (d) Rolls with a branch can be formed with a different initial condition. Oscillation parameters are  $f = 100$  Hz,  $\Gamma = 32.6$ , and  $V = 5$  mL. Arrows represent the direction of the flow.

tion where the depth of the fluid/container constrains the wavelength of the convection. The critical condition for the onset of convection is independent of the volume and the height of the fluid for a wide range of parameters, and is determined by a newly defined parameter: a non-dimensional stress produced by the inertia of the fluid interacting with the oscillating plate.

The experimental apparatus consists of a horizontal aluminum plate (120 mm diameter), mounted on a vi-

bration device (VG-100C: Vibration Test System). The plate is vertically vibrated with a sinusoidal oscillation with amplitude  $A$  and frequency  $f$ , *i.e.*  $z = A \sin(2\pi ft)$ , by a function generator (NF 3540). The dimensionless acceleration amplitude is defined as  $\Gamma = A(2\pi f)^2/g$ , where  $g$  is the gravitational acceleration. The acceleration amplitude of the plate is measured by an accelerometer (PV-90B:RION) to an accuracy of  $\pm 0.2 \text{ m/s}^2$ . The motion is recorded by a high speed CMOS camera with a  $1024 \times 1024$  pixel resolution and time resolution of  $1/1000\text{s}$ . We used fluids with a monotonically shear-thinning property above the yield stress strength, *i.e.* viscoplastic. We report the results for a typical shear-thinning fluid gel (sol-gel intermediate), commonly used for ultrasound examinations (Dane-gel R1, Rohd  products). The material is made of a polymeric gelling agent and water. However, we observed qualitatively similar results using other shear thinning yield stress fluids such as xanthan gum, shaving gel, and toothpaste. We measured the viscosity of the material using a cone plate rheometer with temperature control (Rheosol G5000, UBM). We confirmed that the viscosity decreases with increasing shear rate. We estimated the yield stress of the gel as  $\tau_B \simeq 150 \text{ Pa}$ , using the same device by measuring the maximum stress supported by the gel under constant shear.

A fixed volume of the gel is placed on the plate. The initial shape of the gel is amorphous. The gel is elastically stretched and compressed during the plate oscillation period. As the plate acceleration is increased it becomes apparent that the gel is fluidized, and it rapidly collapses and spreads onto the plate. A lump initially laid on the plate is thus gradually encircled by a rim of inward rotating rolls as the acceleration is increased. The rim of roll elongates in one direction along the horizontal surface breaking the azimuthal symmetry. Within a few seconds the middle part of the lump is invaded by rolls,

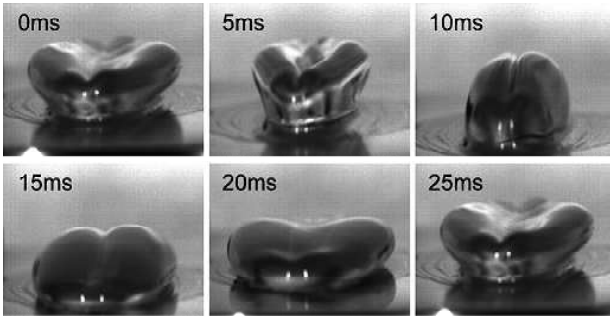


FIG. 2: Side view of the oscillating motion of the rolls at various phases of the plate oscillation ( $f = 40 \text{ Hz}$ ,  $\Gamma = 14.8$ , and  $V = 5 \text{ mL}$ ). Time proceeds from left to right at  $5 \text{ ms}$  intervals. The oscillation of the gel is locked to the plate frequency but out of phase [see Fig. 5(c)]. However, the mean convective flow occurs on a time scale independent of that of the oscillation period.

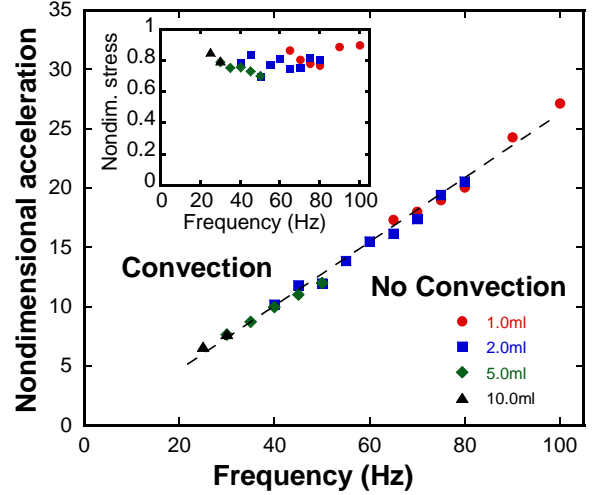


FIG. 3: State diagram of the materials as a function of acceleration and frequency. The fitted line shows the state boundary. Below the line the rolls do not rotate. Above the line they can rotate if the roll shape has been clearly formed. The dashed line is obtained by a linear fit. Inset: The same plot for non-dimensional stress defined by Eq. (1).

and finally become lip-shaped as shown in Fig. 1 (a-b).

Detailed dynamics can be seen with the use of a high speed camera. The rolls oscillate elastically at the same frequency as the plate (shown in Fig. 2) but with a different phase [shown in Fig. 5 (a)]. The gel appears to be folding with each oscillation of the plate. Each roll exhibits inward rotation: outer edges lift from the surface of the plate and fold toward the center of the lump to create rolls as shown in Fig. 2. This motion is very periodic and therefore the net displacement of each part of the fluid is small after each complete period of the oscillation. However, we observe a relatively slow circulating convection within the rolls, by tracking the motions of tracers synchronously with the period of the vertical oscillation. The speed of the convective motion (e.g.  $\sim 1 \text{ Hz}$ ) is much slower than the fast mode of the periodic deformation due to the plate oscillation (e.g.  $40 \text{ Hz}$ ). The motion is independent of the frequency of oscillation but increases as a function of the acceleration of the plate above the onset.

We measure the onset acceleration amplitude  $\Gamma_c$  to determine the dynamical state diagram plotted as a function of frequency, shown in Fig. 3. Once the roll pattern is formed, the shape of the rolls persists even after the vertical vibration is stopped due to the high viscosity and yield stress of the gel. If we decrease  $\Gamma$  from a convecting roll state, rotation of the rolls ceases immediately when  $\Gamma$  becomes lower than the critical value  $\Gamma_c$  and starts as we increase  $\Gamma$  above  $\Gamma_c$  without hysteresis for the onset. The state boundary falls on a line *i.e.*,  $\Gamma \sim (0.27 \pm 0.01)f$ . Therefore the convection starts when the velocity ampli-

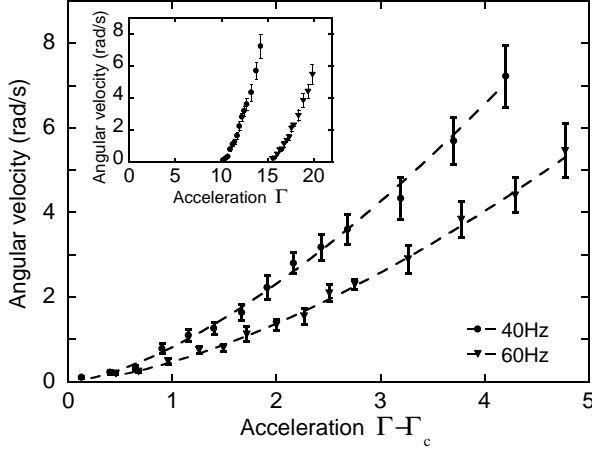


FIG. 4: The mean angular velocity  $\Omega$  as a function of the acceleration above onset,  $\Gamma - \Gamma_c$ . Results for  $f = 40$  Hz with  $V = 5.0$  mL and 60 Hz with  $V = 2.2$  mL. The horizontal axis is shifted such that the onset value  $\Gamma_c$  is at the origin. Each is fit by  $\Omega = \alpha(\Gamma - \Gamma_c)^\beta$ , where  $\alpha$  and  $\beta$  are fit parameters. This results in  $\Omega = (0.82 \pm 0.04) \times (\Gamma - \Gamma_c)^{1.50 \pm 0.04} [\text{s}^{-1}]$  and  $\Omega = (0.47 \pm 0.02) \times (\Gamma - \Gamma_c)^{1.55 \pm 0.03} [\text{s}^{-1}]$ . Inset: The same plot without subtracting  $\Gamma_c$ .

tude  $v = A(2\pi f)$  is larger than a certain threshold velocity  $v_c = 0.39\text{m/s}$ . This threshold varies with different kinds of testing materials. Therefore it is reasonable to introduce non-dimensional parameters in order to clarify the mechanism of the onset of convection. Here we introduce a non-dimensional parameter, a stress exerted by the plate due to the inertia of the material normalized by the yield stress  $\sigma_y$ ,

$$\Sigma \equiv \frac{\sigma}{\sigma_y} = \frac{\rho A^2 (2\pi f)^2}{\sigma_y}. \quad (1)$$

The stress due to inertia is estimated to be  $\sigma = \rho A \cdot A(2\pi f)^2 = \rho v^2$ , where  $\rho$  is the mass density of the material,  $\Sigma$  is the ratio of the exerted stress and the yield stress. We plot the non-dimensional stress  $\Sigma$  for various volumes of material and various frequencies, in the inset of Fig. 4. The critical condition for the onset of convection is  $\Sigma \sim O(1)$ . Despite the fact that the estimation of the yield stress has some ambiguity and the stress distribution is not uniform, the data for various different conditions cluster near the line corresponding to  $\Sigma = 0.8$ . The result strongly supports the hypothesis that the convection starts when the stress distribution in the material exceeds the yield stress  $\sigma > \sigma_y$ , *i.e.* above the solid to fluid transition.

We next measure how the mean angular velocity of the convection rolls changes above the onset. Rotation of the rolls is monitored by following small bubbles or density matched tracer particles which are immersed in the gel for visualization. The convection speed of the fluid depends on the location within the convecting rolls. The

rolls rotate faster in the middle part and slower at the ends. The mean angular velocity (radian/sec) near the mid point of the rolls is obtained from the measurement of the time interval required for several complete cycles of the tracers. The result is shown in Fig. 4. The errorbars in Fig. 4 are relatively large due to the intrinsic angular velocity distributions in the rolls as well as statistical variation. We find that the mean angular velocity increases as an increasing function of the plate acceleration  $\Gamma$  above the onset and is proportional to  $(\Gamma - \Gamma_c)^{1.53 \pm 0.03}$ .

Now we note an important feature of the convecting rolls: The diameter, not the length, of the convective rolls is spontaneously selected. This is particularly true when the frequency of the plate is relatively low. *i.e.* 30Hz – 40Hz. Figure 5(a) shows the time evolution of the diameter of one roll observed from above using the high speed camera. We obtain Fig. 5 (b-c) by plotting the maximum and the minimum observed roll diameter dependence on acceleration and volume. The maximum and the minimum values for the diameter of the rolls are independent of acceleration and volume well above the onset, and for sufficient volume of the material at lower frequencies, *e.g.*  $f \sim 40$  Hz. For higher frequencies, *e.g.*  $f \sim 80$  Hz, the diameter of the rolls is affected by factors such as the initial conditions, suggesting that the stability band of the wavelength selection is wider for higher frequency. We can observe very narrow rolls for the same volume of the material compared with that at

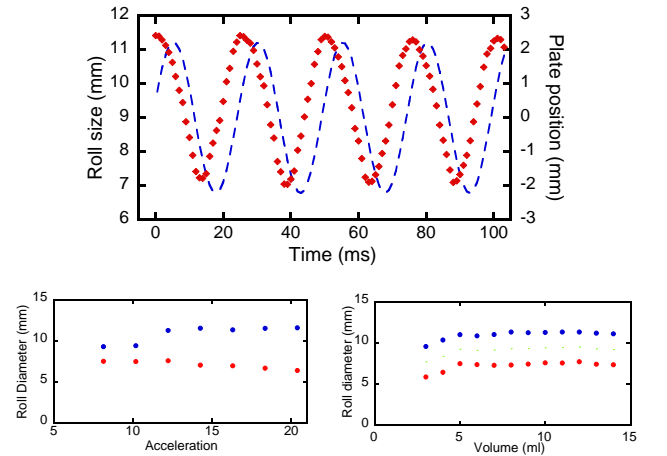


FIG. 5: (a) Dotted line: Time evolution of the diameter of a single roll as observed from above, looking down onto the plate, for  $f = 40$  Hz,  $V = 5$  mL, and  $\Gamma = 14.3$ . Solid line: Position of the plate showing the phase difference. (b) Dependence of the range of roll diameters on acceleration  $\Gamma$  for  $f = 40$  Hz,  $V = 5$  mL ( $\Gamma_c = 10.1$ ). The upper (lower) dots show the maximum (minimum) value of the measured diameter. Note that there is a plateau region for the maximum of the diameters when the acceleration  $\Gamma$  is well above the onset value  $\Gamma_c$ . (c) Size dependence of the roll on the volume of the material measured for  $f = 40$  Hz,  $\Gamma = 12.3$  (above  $\Gamma_c$ ).

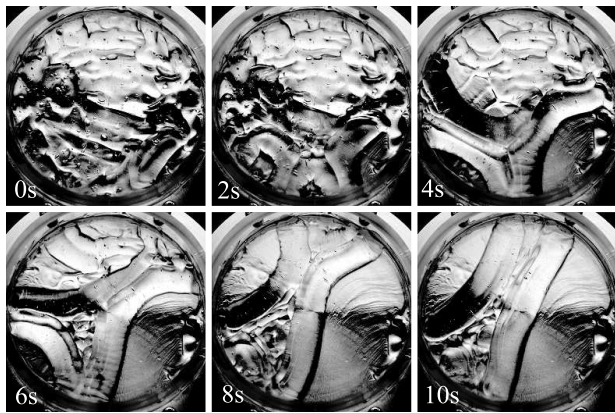


FIG. 6: Aggregation of the gel in a vertically vibrated cylindrical container (acrylic resin walls and aluminum plates). Time proceeds from left to right at intervals of 2 s. The gel eventually gathers into one area enclosed by rolls and the wall, vacating the other areas. The experimental parameters are fixed at  $f = 50$  Hz,  $\Gamma = 27.3$ , and  $V = 25$  mL.

low frequencies. We also note that pattern selection has some initial condition dependence as is typical of other pattern forming phenomena far from equilibrium. For example, a triangular vertex of roll pair or a concentric ring of roll were observed as shown in Fig. 1(c-d), by imposing different initial conditions.

The measurements described until this point were conducted on a freestanding blob of gel on a horizontal plate without sidewalls. However, convection of the gel still occurs in the presence of sidewalls. When placed in a container, the gel self-segregates into a “material sea” region and a “dry” region, with convection rolls forming the “shores”. This process is shown in Fig. 6. An initially uniform shallow (depth of about 15-20 mm) layer of the gel was placed covering the bottom plate of the cylinder. As the plate acceleration is increased above the critical acceleration, a roll eventually forms near the wall. Once a roll forms, it aligns itself perpendicular to the point of contact with the wall (see Fig. 6). The roll tends to straighten and thus the action of the roll is to peel the gel from the bottom plate and move it away from the wall. A very thin layer of gel remains stuck to the plate in the vacated region. Eventually the gel is thus segregated into two regions: a shallow region bounded by the container wall and rolls, and a much thinner layer of gel in the region vacated by the rolls.

The loss of stability and subsequent transition to the convecting state of a vertically oscillated viscoplastic fluid occur due to the solid to fluid transition, as evidenced by the order unity transition of the nondimensional stress. Above the onset, we suspect that a nonlinear mechanism such as acoustic streaming may be responsible for the emergence of the slow mode from the fast oscillating mode[8, 9]. It is reported that the circulating motion around a vibrating rod in viscoelastic materials is in the opposite direction compared to that in Newto-

nian fluids. The fact that the flow on the center line is directed toward the rod coincides with our observation. However, the observed velocity of our convection and that of acoustic streaming behave very differently as a function of vibration velocity. We also speculate that the anisotropy of viscosity plays a crucial role in this phenomenon. Decrease of viscosity (shear thinning) depends on the shear stress tensor. Since the distribution of the stress is anisotropic, the viscosity coefficients of the fluid are also anisotropic. Once the convection rolls are formed by symmetry breaking, the shear in the azimuthal direction is larger than the longitudinal direction. This results in a smaller viscosity in azimuthal direction compared with the longitudinal one, and this effect may stabilize the motions along the azimuthal directions and straighten the rolls.

The newly found state, freestanding convection, can become a new demonstration for viscoplasticity, the presence of a yield stress in a complex fluid. Similar phenomena can be expected to occur in materials ranging from yield stress fluids to amorphous solids[10, 11, 12] and glassy materials[13, 14]. Furthermore, enhanced mixing due to stretching and folding of the fluids during convection may allow for applications to mixing of such fluids.

We thank T. Kataoka, K. Ito, and M. Shibayama for use of their rheometer, K. Takeuchi and S. Tatsumi for useful discussion and experimental help. This work was supported by a Japanese Grant-in-Aid for Scientific Research from Ministry of Education, Culture, Science, and Technology.

- 
- [1] E.C. Bingham, *Fluidity and Plasticity* (McGraw-Hill Inc., New York, 1922).
  - [2] D.V. Boger and K. Walters, *Rheological Phenomena in Focus* (Elsevier, Amsterdam, 1993).
  - [3] D.F. James, *Nature* **212**, 754 (1966).
  - [4] A. Carré, J.-C. Gastel, and M.E.R. Shanahan, *Nature* **379**, 432 (1996).
  - [5] P.B. Umbanhowar, F. Melo, and H.L. Swinney, *Nature* **382**, 793 (1996).
  - [6] H.M. Jaeger, S.R. Nagel, and R.P. Behringer, *Rev. Mod. Phys.* **68**, 1259 (1996), and references therein.
  - [7] F.S. Merkt, R.D. Deegan, D.I. Goldman, E.C. Rericha, and H.L. Swinney, *Phys. Rev. Lett.* **92**, 184501 (2004).
  - [8] Sir J. Lighthill, *J. Sound Vib.* **61**, 391 (1978).
  - [9] C. Chang and W.R. Schowalter, *Nature* **252**, 686 (1974).
  - [10] A. Lemaitre, *Phys. Rev. Lett.* **89**, 195503 (2002).
  - [11] M.L. Falk and J.S. Langer, *Phys. Rev. E* **57**, 7192 (1998).
  - [12] G. Picard, A. Ajdari, F. Lequeux, and L. Bocquet, *Phys. Rev. E* **71**, 010501R (2005).
  - [13] P. Coussot *et al.*, *Phys. Rev. Lett.* **88**, 218301 (2002).
  - [14] F. Varnik, L. Bocquet, J.-L. Barrat, and L. Berthier, *Phys. Rev. Lett.* **90**, 095702 (2003).
  - [15] The movies of the experiments are available at <http://daisy.phys.s.u-tokyo.ac.jp/EC/>.